# Coalitional Dynamic Graph Game for Aeronautical Ad hoc Network Formation

Bing Du, *Member, IEEE,* Xiaomeng Di, Dingming Liu, and Huansheng Ning, *Senior Member, IEEE,*

***Abstract*—Aeronautical Ad hoc Networking (AANET) of the air vehicles is envisioned to support future enhanced applications, such as free flight and in-flight Internet, and AANET serves as the middle layer of the air-space-ground integrated network, bridging the space and the ground components. However, intermittent connectivity is the greatest challenge to an AANET. To deal with the intermittence, the air vehicle acts as a relay in an AANET using the buffer onboard to temporally cache the data when an interruption occurs, known as opportunistic transmission. For the highly dynamic topology of an AANET, we use a sampled dynamic graph to capture significant variations while ignoring trivial changes for avoiding extra complexity. And thus we formulate a coalitional game incorporating with the dynamic graph for the AANET to obtain the optimal transmission schedule in terms of the effective throughput with limited transmission delay. The corresponding coalitional dynamic graph game algorithm will then generate an approximately optimal AANET formation, which converges to Nash equilibrium within finite iterations. The simulations conducted with the real flight data show that 700 Mbit of buffer size onboard and 1400 Mbit of buffer in the Internet Gateway Station (IGS) are the optimal settings for the opportunistic transmission, and the coalitional dynamic graph game algorithm outperforms the geographic location based greedy perimeter stateless routing algorithm in terms of the total received data amounts.**

***Index Terms*—Aeronautical Ad hoc Networking (AANET), opportunistic transmission, dynamic graph, coalitional game.**

## I. Introduction

Over the past several decades, the air transport industry has experienced continuous growth and it is foreseeable that the current air transportation systems will soon be unable to cope with the expected growth in the numbers of air vehicles. As of now, Aircraft Passenger Communications (APC) data service are delivered by Air-to-Ground (A2G) macro-cellular system (e.g., Gogo A2G network) above the continents. When an air vehicle flies over a remote or oceanic area, APC service turns to the aid of Air-to-Satellite (A2S) communications, which implies skyrocketing costs and considerable delays. However, the demand of APC calls for an innovative paradigm to enable an Internet-like surfing experience for the passengers in an air vehicle.

Recently, Aeronautical Ad hoc Networking (AANET) [1]–[3] has been envisioned to support not only fundamental applications such as air traffic control and flight data, but also embrace enhanced applications, such as free flight and in-flight entertainment. AANET is a large scale, multi-hop wireless mobile ad hoc network (MANET) [4] of the air vehicles connected via long range highly directional air-to-air radio links [5]–[8]. The studies in [9] showed that only a minority of the air vehicles being connected directly with the ground stations during long haul of flight, and the AANET is capable of connecting most of the remaining air vehicles (58.3%) over the oceanic airspace. The key enabler is the Air-to-Air (A2A) transmission: the two air vehicles within the communication range of each other can exchange information directly. Thus, A2A has flexible coverage, reduced cost and reduced latency compared with the current A2G networks and A2S communications.

Although AANET serves as the middle layer of the air-space-ground integrated network, naturally bridging the space and ground components, AANET has always been absent and ignored in the air-space-ground integrated network. For investigating the throughput of an AANET, Tu et al. established a multihop AANET with the pseudolinear sequential air vehicles in the Atlantic corridor [7] . Further, [2] proved that the throughput of the AANET can achieve 68.2 kb/s with 1 Mb/s of relaying capacity. [10] further derived the upper bound of the throughput and the closed-form of the average delay for a two-hop aeronautical network. And in [11], the throughput that an air vehicle can reach via the AANET for video, data and voice is 768 kb/s, 197.6 kb/s and 870.41 kb/s, respectively. In particular, for video service, only 2 channels are provided, which is far from sufficient for the ever-increasing demand nowadays.

However, the AANET faces unique challenges [12]–[14]. The mobile nature of the air vehicles, the high velocity (245 m/s $\sim$ 257 m/s en route) and the long transmission range (200 nm for A2G and 400 nm for A2A) often lead to intermittent links, frequent node dropouts, unstable connectivity and variant transmission delays in the AANET. Therefore, it is essential to evaluate the significant performance with these unique challenges and further to find appropriate countermeasures.

NASA/FAA/EUROCONTROL investigated the QoS of future aeronautical communication, which led them conclude

B. Du is with the school of Computer and Communication Engineering, University of Science and Technology Beijing, Beijing, China (e-mail: dubing@ustb.edu.cn).

X. Di is with the school of Computer and Communication Engineering, University of Science and Technology Beijing, Beijing, China (e-mail: s20170680@xs.ustb.edu.cn).

D. Liu is with the school of Computer and Communication Engineering, University of Science and Technology Beijing, Beijing, China (e-mail: liudingming@baosight.com).

H. Ning is with the school of Computer and Communication Engineering, University of Science and Technology Beijing, Beijing, China (e-mai: ninghuansheng@ustb.edu.cn).

This work was supported by the National Nature Science Foundation of China (U1633121 and 91438207) and the Chinese Postdoctoral Science Foundation 2020M670331).

This article has been accepted for publication in a future issue of this journal, but has not been fully edited. Content may change prior to final publication. Citation information: DOI 10.1109/JIOT.2021.3076087, IEEE Internet of Things Journal



that the one-way transmission latency for oceanic/remote/polar area can tolerate 5.9 seconds [15]. Thus, we extrapolate the delay tolerant transmission [16] to the AANET scenario to cope with the intermittent links. Earlier, opportunistic transmission coupled by the delay tolerant concept has been extensively developed in the area of Vehicular ad hoc network (VANET) [17] and unmanned aerial vehicular (UAV) ad hoc network (FANET) [18]. However, the AANET exhibits notably different characteristics with the VANET or the FANET in terms of the node's mobility, throughput requirement and channel model. Martínez-Vidal et al. proposed a delay-tolerant network architecture for an AANET, which combined opportunistic and satellite communication systems by using 2,500 real traces of transatlantic flights [19]–[21]. Vey etc. proved that the delay tolerant concept can improve the connectivity of the AANET over the French sky and over the Atlantic ocean [2].

Regarding the APC service, an AANET should meet the requirement of high-rate Internet access for hundreds of passengers in the cabin of a commercial air vehicle [22]. We assume that all the APC data will be uploaded to the AANET through the Internet Gateway Stations (IGSs) located on shore. Due to the highly dynamic mobility and large-scale geographic distribution of the air vehicles, an AANET suffers from the unstable connectivity and randomly relaying nodes [3]. On one hand, frequent on-and-off A2A link status may arouse unbalanced traffic load, because the traffic is more easily aggregated on the connected A2A links, which leads to the congestion and high probability of the packet loss. On the other hand, randomly relaying nodes may result in variant transmission delays at the air vehicle receivers. To solve the above two problems, an AANET should bear intermittent connections instead of avoiding it exhaustively. Therefore, in this paper, we aim to enable A2A opportunistic transmissions and find the optimal transmission paths in terms of the transmitted data amounts and the transmission delay using a coalitional game, which is a topic of great concern [23], [24] for formulating a non-linear problem.

The selections of the multiple paths of the data flow from the IGSs on shore to the air vehicle receivers are the problem of the formation of an AANET, which is obviously a non-linear problem. In our proposed coalitional graph, the nodes along the transmission path from the IGS to a particular air vehicle receiver form a coalition, in which the nodes are interconnected with each other. The utility of the coalition not only depends on the nodes within the coalition, but also depends on the interconnections among them. Such coalitional game is called coalitional graph game [23], [25]–[27]. In [26], the coalitions of the fixed relay stations were constructed to serve the base station during the uplink transmission, resulting in the lower multi-hop delays. Zhao et al. proposed a coalitional graph game framework for device-to-device (D2D) communication [27]. However, these studies provide us with good references, but they are not suitable for the AANET with high-speed variable topology.

Considering the highly dynamic topology that an AANET exhibits, we use a dynamic graph to capture the variation of the AANET topology. Herein, for a peak scenario of more than 500 air vehicles in the oceanic airspace, we incorporate a coalitional game with a dynamic graph to devise a coalitional dynamic graph game for the AANET. Further, in this coalitional dynamic graph game, we analyze the effective throughput, transmission delay, transmission modes, buffer size onboard and buffer size in the IGS and deduce the optimal settings. To the best of our knowledge, opportunistic transmission in an AANET has been rarely addressed in the literature previously. For clarity, the main contributions are summarized as follows.

- Considering opportunistic transmissions, we adopt the delay tolerant transmission and utilize the buffer onboard to cache the data on the intermittent link. By simulations, we obtain that the optimum buffer size onboard is 700 Mbit. Besides, with 1400 Mbit of buffer in the IGS, the throughput of a single air vehicle can achieve 865.4 Kbit/s, which satisfies the requirement for the video transmission of the APC service [11].
- The key parameter of the dynamic graph is given, so that the dynamic graph can capture the significant topology variations, while ignore the trivial changes for avoiding extra computing complexity.
- We formulate a coalitional dynamic graph game for an AANET. When the network scale is larger than 500 nodes, the AANET formation converges to Nash equilibrium only after finite iterations.
- Compared with the location based greedy routing algorithm, the coalitional dynamic graph game algorithm can make full use of the AANET network resources and perform better. When the bandwidth or the buffer increases, the received data amounts increase more than that of the greedy routing.

The rest of this paper is organized as follows. In section II, we present the system model, the dynamic graph model, and the three possible transmission modes. Section III is devoted to establish the coalitional dynamic graph game framework and the corresponding algorithm is given. Performance evaluations are investigated in Section IV, and Section V concludes this work.

## II. SYSTEM MODEL

In this section, we first describe the characteristics of the AANET. Then, the dynamic graph is used to model the AANET topology, which is generated by the realistic trans-Atlantic flight trajectories. Finally, the three possible transmission modes of the AANET are given.

### A. Network Characteristic

In this paper, we assume that all air vehicles are equipped with A2A link transceivers. Fig. 1 is a snapshot of the AANET created by the realistic trans-Atlantic flight trajectories, which was collected on the $18^{th}$ Sep. 2017 from a flight data company — Official Airlines Guide (OAG). In addition to the characteristics of the conventional wireless ad hoc networks, i.e., distributed computing, self-organizing, multi-hop, and others, an AANET has its own distinctive features as listed below:

- *High mobility and highly dynamic topology*

This article has been accepted for publication in a future issue of this journal, but has not been fully edited. Content may change prior to final publication. Citation information: DOI 10.1109/JIOT.2021.3076087, IEEE Internet of Things Journal



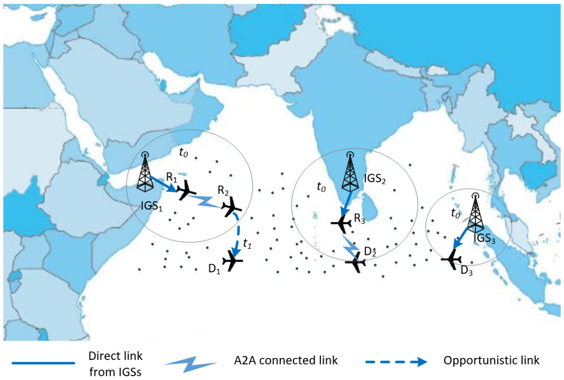


Fig. 1. The scenario of three transmission modes of AANET.

An air vehicle usually moves at a very high speed, i.e., approximately 900 km/h en route, resulting in a highly dynamic topology, which implies that an aircraft node may join or leave an AANET frequently. Thus, an A2A link may suffer from a frequent on-off situation, and the dynamic graph model is adopted to cope with all these variations.

- *Long span and regular movement*
  Generally, a large passenger air vehicle in an AANET experiences a long haul and a wide route distribution. For instance, the single-hop radius can possibly reach hundreds of kilometers, and the coverage of the AANET can probably span the entire ocean. Since the air vehicle always flies along the predefined air route instead of randomly moving, the 3-D position of the air vehicle can be predicted precisely through navigation equipment (i.e., Global Navigation Satellite System). We can thus establish a real time AANET topology with these position data.
- *Hierarchical network structure*
  An AANET contains at least two layers: one is the ground layer including the IGSs located on the ground along the air route or onshore, and the other is the airborne layer including the air vehicles flying above the clouds. The two layers are connected by the A2G links between the gateway nodes of the two layers. In the airborne layer, some of the air vehicles are acting as relays, thus an IGS can be connected to a particular air vehicle receiver in the AANET by both A2G and A2A links. The maximum distance of A2G or A2A depends on the flight altitude and the curvature of the earth surface under the Line-of-Sight (LoS) assumption. For instance, the flight altitude en route is between FL310 and FL400, and the communication range of an A2A can reach 250 nm, while that of an A2G link can reach 200 nm [28].

## B. Dynamic Graph

Attributed to the characteristics of the AANET mentioned above, we use a dynamic graph to model such an AANET, which is a time-expanded graph with a sequence of updates [29]. The update indicates an operation that inserts or deletes edges or vertices in the graph, capturing the behavior of the highly variant topology that AANET exhibits. The basic idea of the dynamic graph is to decompose a variant graph into a few consecutive quasi static sub-graphs along the time course by sampling. We establish the AANET dynamic graph with the predicted air vehicle positions derived from the real flight trajectories. The key factor of the dynamic graph is the sampling interval used to decompose the dynamic graph. For example, if the interval is too long, the significant changes of the AANET topology might be missed. If the interval is too short, the dynamic graph contains too many trivial details, resulting in too much burden on the computing complexity.

Let $\mathbf{H}(t) = \{\mathbf{V}(t), \mathbf{E}(t)\}$ represents the AANET dynamic graph. The vertex set $\mathbf{V}(t)$ consists of the IGSs and all the air vehicle nodes involved. The edge set $\mathbf{E}(t)$ consists of the wireless links between the vertices. The weight of the edge is determined by the wireless link capability. The AANET dynamic topology can expand to several consecutive sub-graphs along the time course. In each of the sub-graphs, the connected relations of the vertices are determined by the physical locations of the air vehicles and wireless transmission constraints. Thus, $\mathbf{H}(t) = \{\mathbf{H}(t_1), \mathbf{H}(t_2), \ldots, \mathbf{H}(t_K)\}$, where $t_k \in \{t_1, t_2, \ldots, t_K\}$ represents the interval index. Due to the wide span of the AANET, during a short interval, the relative physical location of an air vehicle maintains relatively static. We should choose the interval appropriately to satisfy this condition. Therefore, the expansion somehow alleviates the negative impact of the inherent mobility of an air vehicle node in the AANET.

Let $\mathbf{I}$, $\mathbf{R}$ and $\mathbf{D}$ denote the IGS set, the air vehicle relay set and the air vehicle receiver set, respectively. Specically, $\mathbf{I} = \{I_1, I_2, \ldots, I_{n_i}\}$, $\mathbf{R} = \{R_1, R_2, \ldots, R_{n_r}\}$, $\mathbf{D} = \{D_1, D_2, \ldots, D_{n_d}\}$, where $n_i$, $n_r$ and $n_d$ denote the number of the IGSs, the relays and the receivers respectively. Thus, considering the vertices in a sub-graph, $\mathbf{V}(t_k) = \{\mathbf{I}^k, \mathbf{R}^k, \mathbf{D}^k\}$, where the superscript $k$ denotes the $k^{th}$ interval. Regarding the edges in a sub-graph, i.e., $e\left(I_i^k, R_j^k\right)$ represents a directional A2G link from the IGS $I_i^k, I_i^k \in \mathbf{I}^k$ to the relay $R_j^k, R_j^k \in \mathbf{R}^k$. Likewise, $e\left(R_i^k, D_j^k\right)$ represents a directional A2A link from the relay $R_i^k, R_i^k \in \mathbf{R}^k$ to the receiver $D_j^k, D_j^k \in \mathbf{D}^k$.

All the air vehicles are assumed to fly along a predefined air route and we generate the topology at any given time based on the real Air Traffic Service (ATS) flight data. Here, we define an indicator to describe the variation of the AANET topology. Let $N_E(\cdot)$ be the number of edges in the graph, and the indicator $\eta$ represents the change rate of two different sub-graphs in terms of the edge, as defined in (1).

$$\eta_k = \frac{N_E\Bigg(\mathbf{H}(t_{k+1}) - \mathbf{H}(t_k)\Bigg)}{N_E\Bigg(\mathbf{H}(t_k)\Bigg)} \tag{1}$$

In (1), the number of the updated edges between the two consecutive sub-graphs is calculated by $N_E\Bigg(\mathbf{H}(t_{k+1}) - \mathbf{H}(t_k)\Bigg)$. The change rate is thus calculated by $\eta_k$. In order to realize that each of the sub-graphs maintains approximately static, $\eta_k$ is required to be less than $1\%$. Therefore, we can determine the duration of the sampling interval by the condition,

$$t_k = Duration[\eta_k \leq 1\%]. \tag{2}$$

The air vehicles that request the APC data are the receivers, while the other air vehicles that do not request data from the IGSs will act as the relays to help the receivers. As per Fig.1, we will introduce the possible ways to deliver APC data in an AANET. There are 3 IGSs and 6 air vehicles in Fig. 1. 4 air vehicles are within the IGSs coverage and the remaining 2 air vehicles are outside the coverage of the IGSs. The IGSs are connected to the Internet and provide the entire Internet traffic to the AANET. The receiver will obtain the data either through the multi-hop A2A links or the A2G links directly. For example, $R_1$ and $R_2$ are within the coverage of $IGS_1$, but $R_2$ is at the edge of the coverage. $D_1$ is one of the receivers outside the coverage of the IGSs in the Fig.1. Additionally, at the current interval $t_0$, $D_1$ also does not have an active A2A link. Due to the high mobility and opportunistic transmissions, in the next considered interval i.e., $t_1$, $D_1$ may connect to $R_2$ and obtain the required Internet data from $R_2$. Collectively, the data transmission passes through $IGS_1$-$R_1$-$R_2$-$D_1$, in which $IGS_1$-$R_1$ is the direct transmission, $R_1$-$R_2$ is the connected transmission, and $R_2$-$D_1$ is the opportunistic transmission. For the situation of $D_2$, it happens to be on the edge of the macrocell of $IGS_2$ and it has the connected A2A link with $R_3$. Through two hops, $D_2$ can download the content from $IGS_2$. Meanwhile, $D_3$ is lucky to access to $IGS_3$ directly. The three transmission modes illustrated in Fig.1 are concluded as follows.

- *A2G Direct Transmission (DT)*
  In A2G Direct Transmission, the destination directly connects to an IGS when it is within the coverage of the IGS. For example, during the interval $t_0$, $D_3$ is within the coverage of $IGS_3$, so $D_3$ can obtain the data from $IGS_3$ directly. Using DT, the transmission happens in one sub-graph. The DT mode is the ideal transmission mode which has the least transmission delay.
- *A2A Connected Transmission (CT)*
  In A2A Connected Transmission, the destination is not within the coverage of the IGSs, and can not connect to the IGS directly. In this case, the destination needs to use the relay to transmit the data. For example, the paths from $IGS_2$ to $D_2$ use the CT mode. $D_2$ obtains the data with the aid of $R_3$. The transmission rate is limited by the link with the lowest rate in the multi-hops, and the transmission happens in one sub-graph. Therefore, in CT mode, the traffic amounts depends on the transmission time and the transmission rate.
- *A2A and A2G Opportunistic Transmission (OT)*
  Fig.1 shows that in the OT mode, the destination $D_1$ can not connect to the IGSs either with DT or CT in the interval $t_0$; it has to wait for the opportunity to connect to the relay or the IGSs. In the next interval $t_1$, $D_1$ has the opportunity to connect to $IGS_1$ with the aid of $R_1$ and $R_2$. Using OT, the transmission may take place over several intervals. Therefore, the OT mode has the longest transmission delay and the traffic data amounts are limited by the buffer of the relay and the delay constraints.

## III. Coalitional dynamic graph game framework for the AANET Formation

In this section, based on the dynamic graph, we construct a framework of the coalitional game coupled with the dynamic graph to obtain an AANET formation. Specifically, we first propose a utility function that is able to capture the incentives of the nodes to form the coalitions for the transmission in the AANET. Then, we give details on the AANET formation algorithm for the coalitional dynamic graph game. Finally, we prove that the AANET formation algorithm will converge to Nash equilibrium and stay stable.

### A. Utility Function

To better illustrate the role of the utility function, we describe the APC data transmission process from the IGSs on shore to the air vehicle receiver in the oceanic airspace. The requested APC data is cached in the IGSs' buffer in advance and then sent to the multiple air vehicle receivers through multi-hops; thus it is a multi-flow transmission. For analysis, a virtual source $S_v$ and a virtual destination $D_v$ are assumed to attach to the AANET. $S_v$ has the capability of distributing the multi-flow and $D_v$ has the capability of measuring the total received traffic. Usually, the passengers in the air vehicle initiates the request of the APC data. Therefore, in this paper, the AANET formation procedure starts from the receiver which searches for the peripheral IGSs and the relay nodes to form a path to the source $S_v$, resulting in a tree architecture rooted from $S_v$. Assume there are $n_d$ receivers in the AANET corresponding to $n_d$ transmission paths. We formulate a coalitional dynamic graph game to realize this tree-based transmission formation. The nodes along the transmission paths will be the decision players including the IGSs, the relays, and the receivers. Moreover, the nodes in one path, along which a data flow is transmitted to a particular receiver, will collaborate with each other to obtain an optimal transmission mode as to maximize the transmission utility. Let $\mu$ denote the utility function; thus, the coalitional dynamic graph game can be formulated by $G = (\mathbf{I}, \mathbf{R}, \mathbf{D}, \mu)$. We then provide the expression of the utility function that accounts for the performance measures in terms of the received data amounts as well as the transmission delay induced by multi-hop and the opportunistic transmission.

We focus on the performance of the AANET bearing the OT mode, which will significantly affect the received data amounts and the transmission delay at the receiver. Therefore, the utility function is the AANET throughput, which is defined as the ratio of the effective received data amounts to the transmission delay.

Based on the dynamic graph model $\mathbf{H}(t) = \{\mathbf{V}(t), \mathbf{E}(t)\}$, we define the following notion of a path. Each receiver is connected to the IGS through at most one path whenever this path exists. The path between a possible IGS $I_i \in \mathbf{I}$ and the receiver $D_j \in \mathbf{D}$ is defined as a sequence of nodes

$\mathbf{P}(D_j) = \{I_i, R_1, \ldots, R_q, D_j\}$ such that each directed link $e(a_i, b_j) \in \mathbf{E}(t)$, where $a_i, b_j \in \mathbf{V}(t)$. Particularly, there are two categories of the edges in the dynamic graph. One is the edge representing DT or CT which happens within one sub-graph, i.e., $e(a_i^k, b_j^k), k \in \{1, 2, \cdots, K\}$, while the other is the edge representing OT which happens across over two or several sub-graphs, i.e., $e(a_i^k, a_i^{k+1})$. When $e(a_i^k, a_i^{k+1}) \neq 0$, it means that the node $a_i$ can not connect to the receiver by CT or DT modes currently and has to cache the data in the buffer onboard waiting for the OT.

Considering the aeronautical environment, the transmission suffers from high Bit Error Rate (BER). Therefore, the received data amounts of a receiver has to account only for the successful transmissions. Here, we define the effective received data amounts $F_{et}$ as follows,

$$F_{et}(D_j) = \left(1 - BER_{\mathbf{P}(D_j)}\right) \times F(D_j). \tag{3}$$

In (3), $F_{et}(D_j)$ represents the effective traffic flow received by the receiver $D_j$ and $F(D_j)$ is the traffic flow transmitted to the receiver. $BER_{\mathbf{P}(D_j)}$ is the bit error rate at $D_j$ calculated by all the concatenated intermediate relay nodes from an IGS to the receiver.

The transmission delay between the IGS $I_i$ and the receiver $D_j$ is denoted by $\tau(D_j)$. We thus define a utility of a transmission path $\mathbf{p}(D_j)$ by incorporating the effective traffic flow with the transmission delay, as in (4).

$$\mu\Big(\mathbf{p}(D_j)\Big) = \frac{F_{et}(D_j)^{\beta}}{\tau(D_j)^{(1-\beta)}} \tag{4}$$

where $\beta \in (0, 1)$ is a tradeoff parameter. As $\beta$ decreases, the APC services are more sensitive to the transmission delay than the traffic data amounts. The parameter $\beta$ depends on the requirements of the APC Quality of Service (QoS).

Next, we give the expression of the $BER_{\mathbf{P}(D_j)}$ in (3), which is given by the tight upper bound in [30] for the decoded relaying multi-hop diversity channel.

Let $n_{D_j}$ be the total number of the hops of $\mathbf{P}(D_j)$. $\mathbf{P}(R_{j-1})$ is the set including all the terminals that possibly transmit the data to the relay $R_j$ in the path $\mathbf{P}(D_j)$. Let $\mathbf{P}(D_{j,tml}) = \mathbf{P}(D_j) \backslash \{I_i\}$ be the set of all receiving terminals in the path $\mathbf{P}(D_j)$, where $I_i$ represents the possible IGS. Then according to [30], $BER_{\mathbf{P}(D_j)}$ can be calculated by

$$BER_{\mathbf{P}(D_j)} \leq \sum_{R_q \in \mathbf{P}(D_{j,tml})} \frac{1}{2} \left\{ \sum_{R_k \in \mathbf{P}(R_{q-1})} \left[ \prod_{\substack{R_l \in \mathbf{P}(R_{q-1}) \\ R_l \neq R_k}} \frac{\gamma_{R_k,R_q}}{\gamma_{R_k,R_q} - \gamma_{R_l,R_q}} \times \left(1 - \sqrt{\frac{\gamma_{R_k,R_q}}{\gamma_{R_k,R_q} + 1}}\right) \right] \right\}, \tag{5}$$

where $\gamma_{a_i,a_j}$ is the the received SNR (Signal-Noise Ratio) at node $a_j$ from node $a_i$ and can be calculated as follows,

$$\gamma_{a_i,a_j} = p_{DD} - L_{FS} - N_0 - B_w. \tag{6}$$

In (6), $p_{DD}$ is the transmission power of node $a_i$, $N_0$ is the noise variance, and $B_w$ is the transmission bandwidth. $L_{FS}$ (in dB) can be calculated by (7) [21].

$$L_{FS} = 32.44 + 20\log(f_c) + 20\log\left(d_{a_i,a_j}\right), \tag{7}$$

where $f_c$ is the operating frequency and $d_{a_i,a_j}$ is the Euclidean distance between $a_i$ and $a_j$.

Regarding the DT transmission mode, the receiver $D_j$ is directly connected to the IGS $I_i$ without any intermediate relaying nodes, the $BER_{P(I_i,D_j)}$ can be given by

$$BER_{\mathbf{P}(D_j)} = \frac{1}{2}\left(1 - \sqrt{\frac{\gamma_{D_j}}{\gamma_{D_j} + 1}}\right). \tag{8}$$

Due to multi-hops and OT transmissions, we can not neglect the transmission delay. In (4), the utility function is defined as the ratio of the effective traffic flow to the transmission delay. $\tau(D_j)$ is the transmission time required for each receiver, which can be divided into two parts: the transmission time of CT or DT and the caching time of OT. Here, $Rt_{e(a_i,b_j)}$ is the transmission rate from $a_i$ to $b_j$, which depends of the capacity of the wireless link between them. During the transmission, it is possible that one of the nodes in the path $\mathbf{P}(D_j)$ holds the data as it encounters the intermittent situation, resulting in the extra transmission delay, which depends on the interval with which we sample the dynamic graph. Here, the caching time of the OT mode is limited within 3 intervals; therefore, the transmission delay with the OT mode is as follows:

$$\tau(D_j) = \sum_{\substack{b_j \in \mathbf{P}(D_{j,tml}) \\ a_i \in \mathbf{P}(b_j)}} \frac{F_{et}(b_j)}{Rt_{e(a_i,b_j)}} + \sum_{\substack{e\left(a_i^k, a_i^{k+1}\right) == 1 \\ k \in \{1,2,\cdots,K\}}} \tau^k. \tag{9}$$

Substituting (5) (or (8) of DT) and (9) into (3) and (4), we can obtain the utility for a particular data transmission path.

### B. Network Formation Algorithm

In this subsection, we formulate the coalitional dynamic graph game for the AANET and present the corresponding algorithm. The decision players of the game are the nodes of the AANET, including **I**, **R**, and **D**. A feasible action or strategy that each air vehicle can take is to select the relay nodes and the transmission modes according to the current topology. An air vehicle will select the next hop using the strategy from its available action space, and this action space is the sampled time-expanded dynamic graph. Therefore, an air vehicle will choose the next hop and the feasible transmission mode in this time-expanded dynamic graph. If the receiver is within the coverage of the IGS which having the requested data, the DT mode is thus selected. If the connected links are available, the CT mode is selected. If no connected links are detected, the OT mode is implied. As mentioned in Section II.B, $n_d$ receivers correspond to at least $n_d$ paths. As the nodes in the path have to interact with each other to transmit the data with the expected QoS, these nodes in the path naturally form a coalition due to having the common task and purpose, resulting in $n_d$ coalitions. The gaming is the process that a coalition competes with the others for the transmission resources until a balanced AANET formation is achieved. Since we focus on the whole AANET formation rather than finding a path for a particular receiver, the overall utility of the AANET is more rational than the utility of one specific receiver.

The overall utility of the AANET is defined in (10).

$$\mu(\mathrm{G}) = \sum_{D_j \in \mathbf{D}} \mu\Big(\mathbf{P}(D_j)\Big) \tag{10}$$

Next, we will give the coalitional dynamic graph game algorithm, also known as the AANET formation algorithm (AAFM) in this paper, according to the decision-making rules of maximizing the utility.

*1) Updating Criteria:* The initial starting topology of the AANET is a star-shaped topology. The receivers which are within the coverage of the IGSs on shore are directly connected to the nearest IGSs. Through AAFM, all of the $n_d$ receivers can be connected to the IGSs via $n_d$ paths including one or two transmission modes of DT, CT and OT. The nodes in one particular path to a receiver form a coalition to compete with the other coalitions for the AANET resource under the rule of maximizing the utility. Notably, a relay node can serve multiple source nodes at the same time; however, the more source nodes the relay node serves, the lower the transmission rate is allocated to that source node. Therefore, the relay node can be in the different coalitions at the same time, but provide different available bandwidth for different coalitions. The coalitions thus compete for the available bandwidth of the relay nodes.

During the iterations, the players search the strategy action space for the available connections by changing their paths to update the coalition that might have the higher utility. Regarding the updating criteria, there are two kinds of the criteria: one focuses on the increase of the individual coalition utility and the other focuses on the increase of the overall utility of the AANET. In this paper, we prefer to adopt the overall utility as claimed in (10), because such an AANET formation is able to make full use of the available network resources, and this is more desirable than the predominance of one particular receiver.

Let $G_{prev}$ be the previous iteration of the AANET formation. A path to a particular receiver $D_i$ changes the connection and then forms an updated AANET formation $G_{cur}$. This updating process must meet the following updating criteria:

$$G_{prev} \prec G_{\mathrm{cur}} \Leftrightarrow \begin{cases} \mu(\mathbf{P}(D_i)) \leq \mu(\mathbf{P}^{cur}(D_i)) \\ \mu(G_{prev}) \leq \mu(G_{cur}) \end{cases} \tag{11}$$

The updating criteria show that two conditions must be both met when updating a coalition structure as follows:

- The individual utility of a receiver $D_i$ after the update is no less than the previous value.
- The overall system utility of the updated formation is larger than that of the previous formation.

A historical set $ht\left(\mathbf{p}(D_i)\right)$ is defined for the receiver $D_i$, which contains all the coalitions that $D_i$ had formed before. When the updating criteria are satisfied, we also should ensure that the new formed coalition is not in the historical set $ht(\mathbf{p}(D_i))$. With this historical set, we can avoid the trapping set by prohibiting the repeated appearance of the coalitions, that is, the coalitions in the historical set are the ones which have smaller utilities. In spite of the overall utility we use in the AANET formation, the corresponding algorithm can be implemented in a distributed manner that we only need to calculate the utilities of the updated coalitions in each iteration instead of calculating the utilities of all the coalitions. The distributed manner allows the AANET formation can be done in each of the receivers.

*2) AANET Formation Algorithms:* We propose an AAFM in terms of the overall effective traffic throughput. There are two steps in the AAFM. Step 1 is to establish a dynamic graph for the AANET topology, which has been described in section II.B. Step 2 is the AANET formation procedure. In the beginning, all the receivers in the AANET search the nearest IGS in a non-cooperative manner and thus form an initial coalition structure. Notably, in this initial process, there are situations that some of the receivers can not connect to the IGSs. In this case, these receivers search for the currently idle relays and decide whether to use it and thus group it in the coalition based on the updating criteria. When there are no connectable relays in the sub-graph at this moment, it has to wait for at least one interval to do the same procedure in the next sub-graph. After finite iterations, the overall utility of the AANET will be improved and the coalition structure will change accordingly. The iteration will stop when updating ceases, thus a relatively stable AANET is formed and the maximized coalition benefit is thereupon obtained. Once achieving a stable formation, the optimized resource allocation has been made in terms of the overall transmitted data amounts and the average transmission delay. We conclude the AAFM in Algorithm 1.

### *C. Convergence and Stability*

In this section, we analyze the convergence and stability of the AAFM. For the convergence, the number of IGSs, the receivers and relays participating in the formation of coalitions is limited, i.e., in this case $n_i$, $n_r$ and $n_d$; thus, the convergence of the algorithm can be achieved. The convergence and stability of AAFM are proved as follows:

*Theorem 1:* Starting from the initial topology structure, the coalitional dynamic graph game $G = (\mathbf{I}, \mathbf{R}, \mathbf{D}, \mu)$ provides an AANET formation that can finally converge to Nash equilibrium.

*Definition 1:* Nash equilibrium is a state, in which the formation achieves stable and all the coalitions in the AANET will no longer change at the moment (within the interval of the dynamic graph). In an AANET with Nash equilibrium, the AANET has the maximized overall utility.

Proof. The number of the receivers is given, i.e. $n_d$, so only a limited number of the transmission paths can be generated. In other words, the number of the coalitions is limited. The topology of the AANET is generated by the distributed cone-based topology control algorithm [31], which reduces the number of the neighbours for each air vehicle greatly. In the proposed AAFM, each air vehicle will search the nearby air vehicles that can be connected during the process of the formation. Thus, the number of the relay nodes that each air vehicle can choose to connect to is limited. The time that a

**Algorithm 1** The AANET Formation Algorithm (AAFM)

**Step 1 Establish a dynamic graph for the AANET topology**
**Initialization**;
The entire considered time window $T_{sim}$;
The duration increase step $t_{sp} = 30$ sec;
The number of the sub-graphs $n_t$ = 0;
The continuous dynamic graph $\mathbf{H}_{ndt} = \mathbf{H}(T_{sim})$;
Discretized dynamic graph $\mathbf{H}_{dt} = \{\}$;
Generate discretized sub-graphs
**repeat**
  Set duration $t_{n_t} = 0$;
  **while** Topology change rate $\eta_{n_t} \leq 1\%$ ($\eta_{n_t}$ is calculated by (1)) **do**
    $t_{n_t} = t_{n_t} + t_{sp}$;
  **end while**
  Elapsed time $t_{elp} = t_{elp} + t_{n_t}$;
  The continuous dynamic graph $\mathbf{H}_{ndt} = \mathbf{H}(T_{sim} - t_{elp})$;
  Discretized dynamic graph $\mathbf{H}_{dt} = \{\mathbf{H}_{dt}, \mathbf{H}(t_{n_t})\}$;
  $n_t = n_t + 1$;
**until** $t_{elp} = T_{sim}$
**Output** $\mathbf{H}_{dt} = \{\mathbf{H}(t_1), \mathbf{H}(t_2), \cdots, \mathbf{H}(t_{n_t})\}$
**Step 2 the AANET formation**
**Initialization**;
All of the air vehicle receiver connect to the nearest IGS, forming an initial formation $G_{ini}$;
The overall utility $\mu(G_{ini})$ is calculated by (10);
In the $m^{th}$ iteration, each coalition searches for a better strategy in $\{\mathbf{H}(t_1), \mathbf{H}(t_2), \cdots, \mathbf{H}(t_{n_t})\}$ to obtain a higher overall utility of the AANET;
**repeat**
  One of the receiver $D_j$ updates the path $\mathbf{P}(D_j)$ with the new path $\mathbf{P}^{cur}(D_j)$ randomly;
  A new formation $G_{cur}$ is generated;
  The overall utility $\mu(G_{cur})$ of the new formation is calculated by (10);
  **if** $\mu(G_{cur}) \geq \mu(G_{ini})$ && $\mu(\mathbf{P}^{cur}(D_j)) \geq \mu(\mathbf{P}(D_j))$ && $G_{cur} \notin ht\,(\mathbf{p}(D_i))$ **then**
    Update $\mathbf{P}(D_j) = \mathbf{P}^{cur}(D_j)$;
    Update: $G_{ini} = G_{cur}$; $\mu(G_{ini}) = \mu(G_{cur})$;
    $m = m + 1$;
  **else**
    Remain unchanged;
    $m = m + 1$;
    goto **repeat**
  **end if**
**until** No more updating emerges or $m$ reaches the predefined maximum iterations $M_{itl}$
**Output** the consequent AANET formation

relay caches the data is limited, i.e., each air vehicle caches the data for at most three intervals in the OT mode. The transmission hops are also limited for the practical realizations, for example, the maximum number of the hops for each path is limited within three hops. With all these limitations, the strategy space that each coalition can choose to update is limited. Further, the AAFM introduces the historical set $ht\,(\mathbf{p}(D_i))$ to avoid the trapping set; therefore, the AANET will reach Nash equilibrium after finite iterations within the limited strategy space.

We prove the stability of the proposed AAFM by contradiction. Suppose the coalitions obtained by AAFM are not stable, meaning that there must be a situation that an air vehicle can choose a better strategy by leaving or joining a coalition to improve the overall utility of the AANET. AAFM does not converge under this situation, which contradicts the fact of the Theorem 1. The AAFM will keep searching the strategy space for the better options until it traverses all the available strategies and achieves the maximum overall utility eventually. At this moment, the AANET formation generated by AAFM achieves the Nash equilibrium.

## IV. SIMULATION

In this section, we evaluate the performance of the proposed AAFM to reveal the performance limitations and trade-offs of the delay-constrained AANET. We implemented our experiment with a realistic flight data, which includes the air routes of all commercial airlines worldwide today and 17 ground IGS stations around the North Atlantic. We observed the data in a 24-hour time window and selected the peak hour of 5:00 UTC, at which there was the highest density of the air vehicles in the air. We used the data, including the longitude, latitude, altitude, heading, and speed to generate the corresponding trajectories, which are approximated by the great circle arcs between the departure and the destination airports. Suppose all the air vehicles fly at the same altitude, i.e, 10,000 meters. The airborne topology is generated by the distributed cone-based topology control algorithm [31], which guarantees that each $120°$ cones centered on an air vehicle contains at least one connectable neighbor node. During the considered period, the number of the air vehicle participating in the coalitional dynamic graph game is about 580, which consists of the relays and the receivers. The transmit power is set to 46 dBm for all the air vehicles, the noise level is 100 dBm, and the bandwidth $B_w$ per IGS is set to 10 MHz. We assume that A2A and A2G are sharing the spectrum; that is, A2A will take the bandwidth belonging to A2G whenever A2G is idle [32]. This assumption is reasonable since the frequency band for aeronautical communication is already announced to be crowded and no extra new band can be allocated to the A2A service. For the operating frequency, we use the VHF frequency band and $f_c = 137$ MHz. The simulation settings are summarized in Table 1.

To study the performance of the AAFM, we analyze how the key factors affect the data transmission in the AANET, such as the available bandwidth, buffer size onboard, buffer size of the IGSs and the topology change rate. Fig. 2 shows a snapshot of the AANET formation obtained by the proposed AAFM and the paths from some of the aircraft receivers to the IGSs.

### A. The Impact of the Buffer in the IGSs

The buffer plays an important role in the coalitional dynamic graph game framework, because it affects the performance of

TABLE I
SIMULATION PARAMETERS

| Parameter | Value |
|---|---|
| Sector type | En-Route |
| Air space | trans-Atlantic |
| Operating frequency (MHz) | 137 |
| Maximum transmission rage $d_{A2G}$ (nm) | 200 |
| Maximum transmission rage $d_{A2A}$ (nm) | 250 |
| Total transmitter power (dBm) | 46 |
| Thermal noise density (dBm/Hz) | -164.9 |
| Subchannel interval (kHz) | 25 |
| Bandwidth (MHz) | 10 |
| Pathloss exponent | 2 |
| Flight altitude (m) | 10000 |
| Flight velocity (km/h) | 900 |
| The number destination aircraft | $10 \sim 50$ |
| Number of IGSs on shore | 17 |
| Buffer of the IGS (Mbit) | $100 \sim 1500$ |
| Buffer of the Relay (Mbit) | $100 \sim 1000$ |

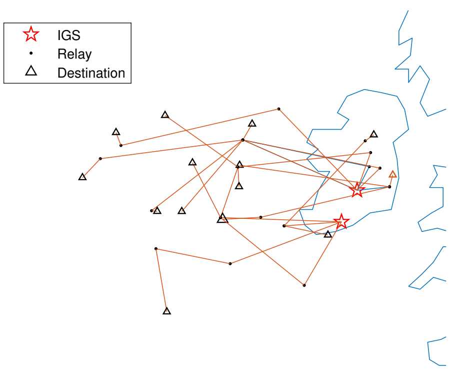


Fig. 2. A snapshot of the AANET formation.

the OT mode. We first investigated how the buffer in the IGSs will affect the AANET formation. In the OT, the IGS needs to buffer the requested data in advance so that the data can be retrieved and transmitted when the links to the receiver are established. A2G has $25\%$ of the total bandwidth and the rest is taken by the A2A transmissions. The buffer in the relay is set to be 500 Mbit. As illustrated in Fig.3(a), the data amounts received will increase with the growth of the buffer in the IGS. Further, the utility of the coalitional dynamic graph game also increases with the growth of the buffer in the IGS when $\beta = 0.8$; the increase rate is about 0.68 Gbit per 100 Mbit on average. Combined with Fig.3(b), we can see that within 1000 Mbit of the IGS buffer, the ratio of OT decreases and the ratio of DT increases, while the ratio of CT randomly changes. This is due to some traffic offloads from the DT mode rather than the OT mode, which is preferred since the transmission delay would be saved. Additionally, the CT mode may have random hops resulting in random traffic load, and we can also see that the CT only takes less than $10\%$, because the intermittent links are dominant in the AANET. Beyond 1000 Mbit of the IGS buffer, the ratio of OT increases and the ratio of DT decreases, which will enlarge the transmission delay. Therefore, the better choice for the buffer of the IGS is 1000 Mbit, with which the average throughput of one single air vehicle can achieve $865.4$ Kbit/s, calculated by (12), which satisfies the requirements for the video transmission of the APC service [11].

$$\frac{\text{Received data amounts}}{\text{Transmitted time} \times \text{Destination air vehicle number}} = \frac{2.3366 \times 10^4 (\text{Mbit})}{540(\text{s}) \times 50} = 865.4 (\text{Kbit/s}). \tag{12}$$

From Fig.3(c), we can conclude that the AAFM can converge to Nash equilibrium within 1000 iterations.

### B. The impact of the Buffer in the Relay

The OT mode needs to use the buffer to cache the data and wait for the opportunity to transmit the data. Thus, the buffer size of the relay is another key factor that will significantly affect the utility of the AANET formation. A2G occupies $25\%$ of the total bandwidth and the rest is taken by the A2A transmissions. The buffer of the IGS is set to be 500 Mbit, and $\beta$ is set to 0.8. As shown in Fig.4(a), when the buffer of the relay is within the range of 100 Mbit to 700 Mbit, with the increase of the buffer size of the relay, the received data amounts also increases, i.e., if the buffer size increases from 200 Mbit to 600 Mbit, the total received data amounts increased by 2000 Mbit. The increase rate is about 0.35 Gbit per 100 Mbit on average. Note that the overall utility is maximized when the buffer size is 700 Mbit. However, when the buffer size of the relay exceeds 700 Mbit, the received data amounts remained almost constant and the overall utility is decreased. From Fig.4(b), we can see that the ratio of OT increases and the ratio of DT and CT decrease. It is because when the buffer size of the relay is enlarged, some of the traffic moves to the OT mode from the DT mode. Obviously, the optimal value of the buffer size of the relay should be 700 Mbit, with which the overall utility has the maximum value. From Fig.4(c), we can observe that with 700 Mbit buffer in the relay, the AAFM converges much faster.

### C. The impact of the Bandwidth and Spectrum Sharing

In this subsection, we investigate how the ratios of the three transmission modes will change with the available bandwidth and spectrum sharing. As shown in Fig.5(a), the received data amounts increases with the total bandwidth; the increase rate is about 1.12 Gbit per 1 MHz of the bandwidth on average. In Fig.5(b), we can observe that the ratios of the three transmission modes remain almost constant. The received data flows transmitted by DT, CT and OT, respectively are given in Fig.5(c). As the total bandwidth increases, the received data amounts by these three modes increase at the same rate. In other words, the change of the bandwidth will not affect the ratios of the three transmissions. In Fig.5(d), we can see that with the increase of the total bandwidth, the convergence slows down.

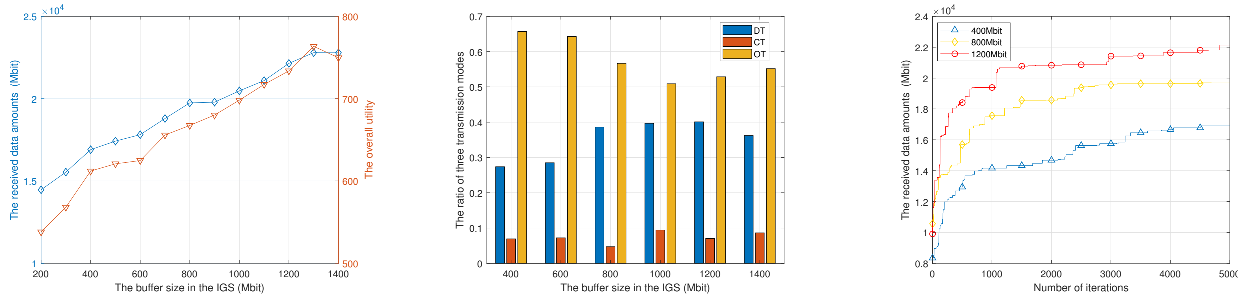


(a) The received data amounts and the utility of the AANET versus the IGS buffer size.

(b) The ratio of DT, CT and OT (with the same parameters).

(c) The iterative numbers of achieving Nash equilibrium.

Fig. 3. The received data amounts and utility versus the IGS buffer size. The total bandwidth is 10 MHz, A2G occupies 25% of the total bandwidth, the buffer size of the relay aircraft is 500 Mbit.

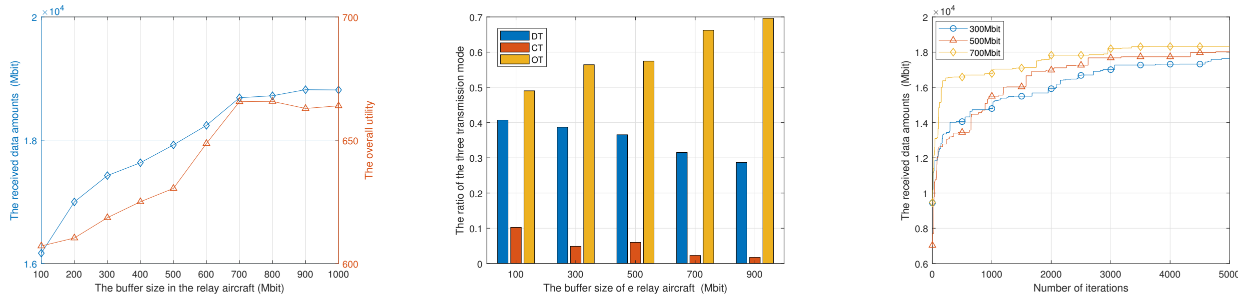


(a) The received data amounts and the utility of the AANET versus the buffer size of the relay.

(b) The ratio of DT, CT and OT (with the same simulation parameter).

(c) The iterative numbers of achieving Nash equilibrium.

Fig. 4. The received data amounts and the utility versus the relay buffer. The total bandwidth is 10 MHz, A2G occupies 25% of the total bandwidth, the buffer size of the IGS is 500 Mbit.

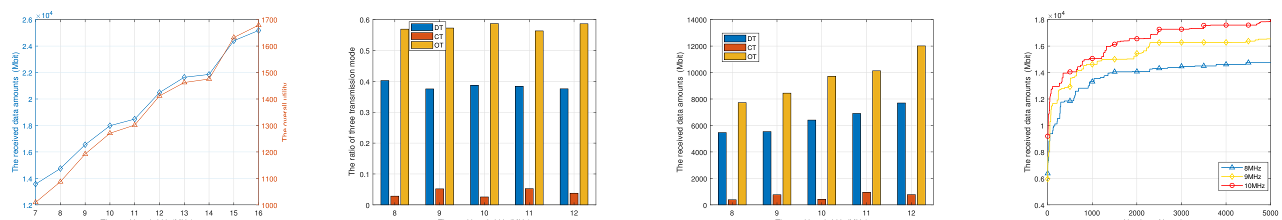


(a) The received data amounts and utility of the AANET versus the total available bandwidth.

(b) The ratio of DT, CT and OT (with the same parameters).

(c) The received data amounts of the three modes.

(d) The iterative numbers of achieving Nash equilibrium.

Fig. 5. The received data amounts and utility versus the total available bandwidth. A2G occupies 25% of the total bandwidth, the buffer size in the IGS and the relay are both 500 Mbit.

We also investigate how the spectrum sharing will affect the performance in Fig. 6. We assume that A2A and A2G are sharing the spectrum and A2A will use the spectrum belonged to A2G whenever possible. In Fig. 6(a), we plotted the curves of the received data amounts and the utility versus the bandwidth taken by the A2G communications. As the proportion of the bandwidth occupied by A2G increases, the received data amounts and the utility both increase, which means the DT mode are desirable among the three transmission modes. However, DT cannot guarantee the seamless service, especially in oceanic airspace. Combining Fig. 6(b) and Fig. 6(c), when the percentage of the A2G bandwidth is less than $40\%$, the data transmitted by OT increases, but it will decrease when A2G occupies more than $40\%$ of the total bandwidth.

### D. The impact of the Dynamic Graph

We use the dynamic graph to model the highly variant topology of the AANET. The key factor of the dynamic graph is the interval that we use to discretize the time course so that during each interval the topology of the AANET can maintain relatively static. The intervals can be decided as per (1). Here, We chose two typical values: 1-min long and 3-min long. Both of them satisfy the (1); 1-min long is more granular, which can catch more details of the variations. However, from

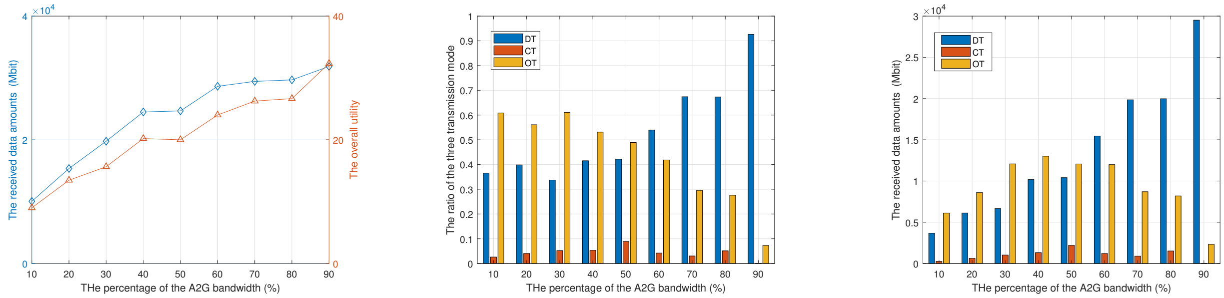


(a) The received data amounts and the utility of the AANET versus the A2G bandwidth.

(b) The ratio of DT, CT and OT (with the same parameters).

(c) The received data amounts of the three modes.

Fig. 6. The received data amounts and the utility versus the A2G bandwidth. The buffer size in the IGS and the relay are both 500 Mbit.

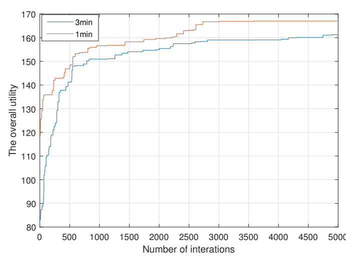


Fig. 7. The impact of the dynamic graph

Fig.7 we can see that the total received data amounts of using 1-min dynamic graph is slightly less than that of using 3-min dynamic graph. According to the simulation results, the difference in the utility between the two values of the interval is only $5\%$. Therefore, it is reasonable for us to choose 3-min long interval to avoid unnecessary trivial variations of the topology.

Then, we investigate how the number of the intervals will affect the data flow of the AANET in Fig. 8. We plotted the curves with 10 intervals. The buffer size of the IGS and the relay is 1000 Mbit and the bandwidth is 10 MHz. The maximum traffic of the entire AANET increases as the transmission time increases. The longer the transmission time is, the higher the OT ratio will be. And the traffic of OT also increases with the growth of the transmission time. As shown in Fig. 8(a), it can be seen that the total received data amounts change similarly as that of OT. From the $3rd$ interval to the $10th$ interval, the overall received data amounts are increased by 7 Gbit and the traffic of OT is increased by 6 Gbit. The increased traffic of OT accounts for 85% of the total increased traffic, which means that most of the increased traffic is transmitted by OT. As illustrated in Fig.8(b), the OT mode is dominant among three transmission modes.

## *E. The Comparison between GPSR and AAFM*

First, we discuss the effect of the tradeoff parameter $\beta$ in Fig. 9. $\beta$ is used in the overall utility as defined in (4). With the increasing of $\beta$, the utility is more sensitive to the received data amounts than to the transmission delay. As shown in Fig. 9(a) and Fig. 9(b), the received data amounts and the transmission delay both grow with $\beta$.

Then, we used the Greedy Perimeter Stateless Routing (GPSR) algorithm as a benchmark, which used the geographic location information in the greedy algorithm for the routing in an Ad Hoc UAV Network [33]. GPSR chooses the next hop based on two principles: strong neighbor connection persistence and shorter distance to the destination, which guarantee the faster forwarding and fewer hops. In Fig.10, we compare the GPSR algorithm with the AAFM algorithm in terms of the received data amounts. Fig. 10(a) plots the received data amounts versus the number of the receivers with respect to GPSR and AAFM. With the increase of the number of the receivers, the AAFM can obtain more improvement, i.e, with 50 receivers, the received data amounts of the AAFM are $1.5$ times that of GPSR. As shown in Fig. 10(b), as the buffer size of the IGS increases, the received data amounts of AAFM is $35\%$ greater than that of GPSR. In Fig.10(c), since GPSR can not bear the OT mode, the traffic is only transmitted by the DT and CT modes. Therefore, when the buffer size of the relay is increased, GPSR has no obvious gain in terms of the overall received data amounts. Therefore, the AAFM performs better than GPSR because of introducing the OT mode, which accounts for the potential of the AANET. In addition, we investigate the convergence performance of the AAFM in Fig. 11, after more than 1500 iterations, the transmitted traffic remains approximately constant, which means the AANET can converge within 1500 iterations.

## *F. Results Summary*

By summarizing and analyzing the simulation results, the following conclusions can be obtained:

- The coalitional dynamic graph game proposed in this paper can converge to Nash equilibrium within a limited number of iterations i.e., within 1500 iterations, when the AANET scale is more than 500 nodes.
- The buffer realizes the opportunistic transmission in an AANET and there exists an optimal size for the buffer design. For instance, using the realistic flight data in the paper, the optimum buffer size of the air vehicle is 700 Mbit. When it is higher than 700 Mbit, there is no significant increase in the total effective throughput. With a 1400 Mbit of buffer in the IGS, the throughput of a single air vehicle can achieve 865.4 Kbit/s, which

This article has been accepted for publication in a future issue of this journal, but has not been fully edited. Content may change prior to final publication. Citation information: DOI 10.1109/JIOT.2021.3076087, IEEE Internet of Things Journal



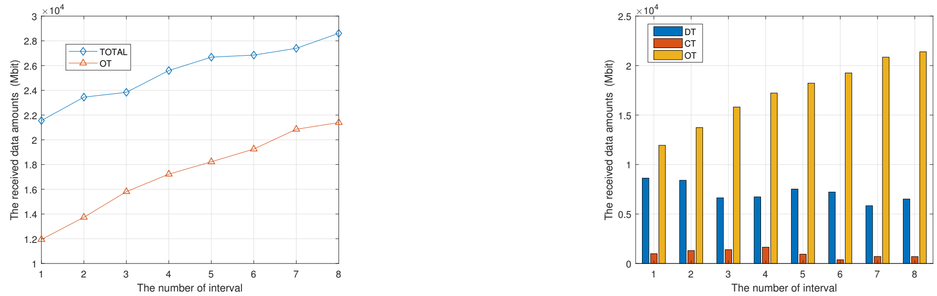


(a) The received data amounts versus the number of the intervals.

(b) The ratio of DT, CT and OT (with the same simulation) parameters.

Fig. 8. The received data amounts versus the number of the intervals. The interval is 3 minutes. The total bandwidth is 10MHz, The A2G occupies 25% of the total bandwidth, the buffer size of the IGS and the relay are both 500 Mbit.

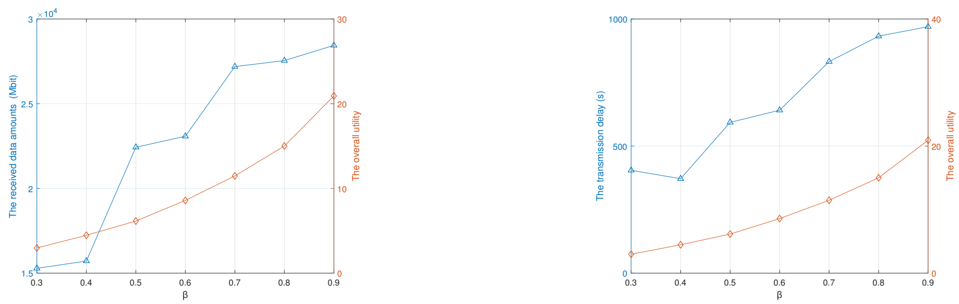


(a) The received data amounts and the utility of the AANET versus $\beta$.

(b) The transmission delay and the utility of the AANET versus $\beta$.

Fig. 9. The received data amounts and the utility versus $\beta$. A2G occupies 25% of the total bandwidth, the buffer size of the IGS and the relay are both 500 Mbit.

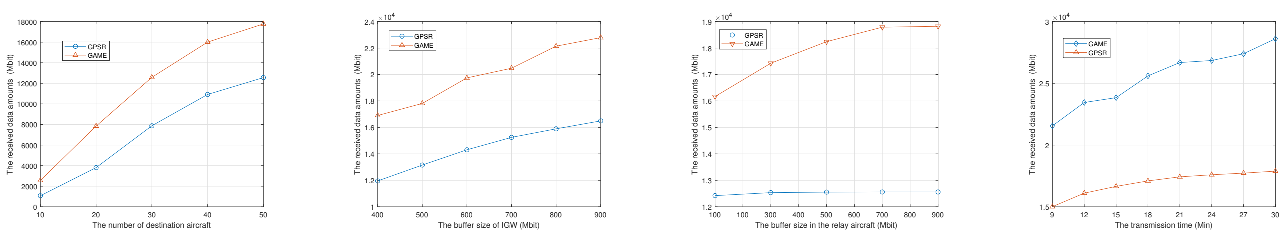


(a) GPSR and AAFM versus the number of the destinations.

(b) GPSR and AAFM versus the buffer size of the IGS.

(c) GPSR and AAFM versus the buffer size of the relay.

(d) GPSR and AAFM versus the transmission time.

Fig. 10. The comparison between GPSR and AAFM. The total bandwidth is 10MHz, A2G occupies 25% of the bandwidth.

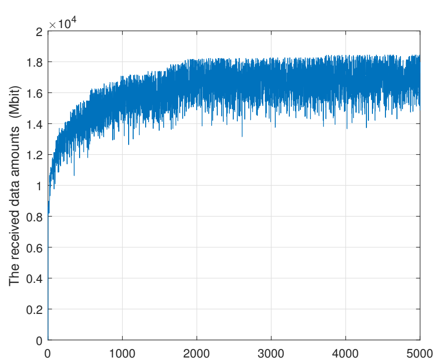


Fig. 11. The convergence of AAFM

satisfies the requirement for the video transmission of the APC service.

- The duration of the interval used to sample the dynamic graph can be set to 3 minutes, which is able to capture the significant variations of the dynamic topology while ignore the trivial changes for avoiding extra computing complexity.
- The AAFM with the same network settings outperforms the GPSR in terms of the received data amounts, for example, the received data amounts of AAFM exceed 18 Gbit, while that of GPSR is about 12 Gbit when the buffer size of the IGS and the relay are both 500 Mbit.

## V. Conclusion

Aiming to solve the problem of the intermittent events in the AANET, this paper formulates a coalitional dynamic graph game to generate a feasible AANET formation that allows the utilization of the opportunistic transmission by utilizing the buffer onboard to temporally cache the data when encountering the intermittent event. A dynamic graph model is built for characterizing an AANET topology, then incorporating with the coalitional game, in which the players and the interactions among them are mapped to the vertices and edges of the dynamic graph. This coalitional dynamic graph game can evolve to Nash equilibrium with finite iterations by maximizing a utility which is measured by the effective throughput of the AANET. Through extensive simulations, the corresponding algorithm AAFM can obtain a feasible transmission path for a particular receiver, and obtain an optimal AANET formation for all the receivers. Compared with the GPSR, the AAFM performs better in terms of the total received data amounts.

With the rapidly development of the LEO satellite constellation, the information services it enables will be cheaper and more common. We will research on the construction of the AANET based on the satellite constellation to provide passengers with more convenient and seamless information services.

## References


[1] J. Zhang, T. Chen, S. Zhong, J. Wang, W. Zhang, X. Zuo, R. G. Maunder, and L. Hanzo, "Aeronautical ad hoc networking for the internet-above-the-clouds," *Proceedings of the IEEE*, vol. 107, no. 5, pp. 868–911, 2019.

[2] Q. Vey, A. Pirovano, J. Radzik, and F. Garcia, "Aeronautical ad hoc network for civil aviation," in *International Workshop on Communication Technologies for Vehicles*. Springer, 2014, pp. 81–93.

[3] D. Medina and F. Hoffmann, "The airborne internet," in *Future Aeronautical Communications*. IntechOpen, 2011.

[4] M. Conti and S. Giordano, "Mobile ad hoc networking: milestones, challenges, and new research directions," *IEEE Communications Magazine*, vol. 52, no. 1, pp. 85–96, 2014.

[5] R. Degenhardt, J. Szodruch, and S. Plass, "Ifar–the international forum for aviation research," in *Future Aeronautical Communications*. IntechOpen, 2011.

[6] D. Medina, F. Hoffmann, S. Ayaz, and C.-H. Rokitansky, "Feasibility of an aeronautical mobile ad hoc network over the north atlantic corridor," in *2008 5th Annual IEEE Communications Society Conference on Sensor, Mesh and Ad Hoc Communications and Networks*. IEEE, 2008, pp. 109–116.

[7] H. D. Tu and S. Shimamoto, "A proposal of relaying data in aeronautical communication for oceanic flight routes employing mobile ad-hoc network," in *2009 First Asian Conference on Intelligent Information and Database Systems*. IEEE, 2009, pp. 436–441.

[8] C. Zhang, Y. Zhang, J. Xiao, and J. Yu, "Aeronautical central cognitive broadband air-to-ground communications," *IEEE J. Sel. Areas Commun.*, vol. 33, no. 5, pp. 946–957, 2015.

[9] M. S. B. Mahmoud, C. Guerber, N. Larrieu, A. Pirovano, and J. Radzik, *Aeronautical Air-Ground Data Link Communications*. Wiley Online Library, 2014.

[10] Y. Wang, M. C. Ertürk, J. Liu, I.-h. Ra, R. Sankar, and S. Morgera, "Throughput and delay of single-hop and two-hop aeronautical communication networks," *Journal of Communications and Networks*, vol. 17, no. 1, pp. 58–66, 2015.

[11] W. Schütz, M. Schmidt, and T. Jacob, "Radio frequency spectrum requirement calculations for future aeronautical mobile (route) system. am (r) s," *LS Telecom AG, Tech. Rep*, 2003.

[12] S. Hayat, E. Yanmaz, and R. Muzaffar, "Survey on unmanned aerial vehicle networks for civil applications: A communications viewpoint," *IEEE Communications Surveys & Tutorials*, vol. 18, no. 4, pp. 2624–2661, 2016.

[13] X. Cao, P. Yang, M. Alzenad, X. Xi, D. Wu, and H. Yanikomeroglu, "Airborne communication networks: A survey," *IEEE Journal on Selected Areas in Communications*, vol. 36, no. 9, pp. 1907–1926, 2018.

[14] J. Liu, Y. Shi, Z. M. Fadlullah, and N. Kato, "Space-air-ground integrated network: A survey," *IEEE Communications Surveys & Tutorials*, vol. 20, no. 4, pp. 2714–2741, 2018.

[15] T. Gilbert, J. Jin, B. Jason, and S. Henriksen, "Future aeronautical communication infrastructure technology investigation," 2008.

[16] V. Cerf, S. Burleigh, A. Hooke, L. Torgerson, R. Durst, K. Scott, K. Fall, and H. Weiss, "Delay-tolerant networking architecture," Tech. Rep., 2007.

[17] P. R. Pereira, A. Casaca, J. J. P. C. Rodrigues, V. N. G. J. Soares, J. Triay, and C. Cervello-Pastor, "From delay-tolerant networks to vehicular delay-tolerant networks," *IEEE Communications Surveys Tutorials*, vol. 14, no. 4, pp. 1166–1182, Fourth 2012.

[18] A. Mukherjee, N. Dey, R. Kumar, B. K. Panigrahi, A. E. Hassanien, and J. M. R. S. Tavares, "Delay tolerant network assisted flying adhoc network scenario: modeling and analytical perspective," *Wireless Networks*, vol. 25, no. 5, pp. 2675–2695, Jul 2019.

[19] R. Martínez-Vidal, R. Martí, C. J. Sreenan, and J. Borrell, "Methodological evaluation of architectural alternatives for an aeronautical delay tolerant network," *Pervasive and Mobile Computing*, vol. 23, pp. 139–155, 2015.

[20] R. Martínez-Vidal, R. Martí, and J. Borrell, "Analyzing information propagation in a transoceanic aircraft delay tolerant network," in *39th Annual IEEE Conference on Local Computer Networks*. IEEE, 2014, pp. 116–123.

[21] R. Martínez-Vidal, R. Martí, and J. Borrell, "Characterization of a transoceanic aircraft delay tolerant network," in *38th Annual IEEE Conference on Local Computer Networks*, Oct 2013, pp. 565–572.

[22] J. Zhang, S. Chen, R. G. Maunder, R. Zhang, and L. Hanzo, "Adaptive coding and modulation for large-scale antenna array-based aeronautical communications in the presence of co-channel interference," *IEEE Transactions on Wireless Communications*, vol. 17, no. 2, pp. 1343–1357, 2017.

[23] W. Saad, Z. Han, M. Debbah, A. Hjorungnes, and T. Basar, "Coalitional game theory for communication networks," *IEEE Signal Processing Mag.*, vol. 26, no. 5, pp. 77–97, 2009.

[24] P. Herings, G. van der Laan, and D. Talman, "Cooperative games in graph structure," 2000.

[25] W. Saad, Z. Han, T. Basar, M. Debbah, and A. Hjorungnes, "Coalition formation games for collaborative spectrum sensing," *IEEE Trans. Veh. Technol.*, vol. 60, no. 1, pp. 276–297, 2011.

[26] ——, "Network formation games among relay stations in next generation wireless networks," *IEEE Trans. Commun.*, vol. 59, no. 9, pp. 2528–2542, 2011.

[27] Y. Zhao, Y. Li, Z. Ding, N. Ge, and H. V. Poor, "A coalitional graph game framework for network coding-aided d2d communication," *EURASIP Journal on Advances in Signal Processing*, vol. 2016, no. 1, p. 2, 2016.

[28] F. Hoffmann, D. Medina, and A. Wolisz, "Optimization of routing and gateway allocation in aeronautical ad hoc networks using genetic algorithms," in *Wireless Communications & Mobile Computing Conference*, 2011.

[29] C. Demetrescu and P. Italiano, *Dynamic graphs, Handbook on Data Structures and Applications*. New York: CRC Press Series, in Computer and Information Science, 2005.

[30] J. Boyer, D. D. Falconer, and H. Yanikomeroglu, "Multihop diversity in wireless relaying channels," *IEEE Transactions on communications*, vol. 52, no. 10, pp. 1820–1830, 2004.

[31] L. Li, J. Y. Halpern, P. Bahl, Y. M. Wang, and R. Wattenhofer, "A cone-based distributed topology-control algorithm for wireless multi-hop networks," *IEEE/ACM Transactions on Networking*, vol. 13, no. 1, pp. 147–159, 2005.

[32] B. Du, R. Xue, L. Zhao, and V. C. Leung, "Coalitional graph game for air-to-air and air-to-ground cognitive spectrum sharing," *IEEE Transactions on Aerospace and Electronic Systems*, vol. 56, no. 4, pp. 2959 – 2977, 2020.

[33] L. Lin, Q. Sun, S. Wang, and F. Yang, "A geographic mobility prediction routing protocol for ad hoc uav network," in *Globecom Workshops*, 2012.

**Bing Du** received her B.S. degree in 2002, and Ph.D. degree in 2009 both from Beijing University of Aeronautics and Astronautics, China. From 2010 to 2014, she worked as an Assistant Researcher in the Department of Electronic Engineering, Tsinghua University.

Since 2015, she has been with the school of Computer and Communication Engineering at University of Science and Technology Beijing, where she is currently an Assistant Professor. Her research interests mainly focus on aeronautical communications, datalink, network coding, cooperative communications, and cognitive radio.

**Xiaomeng Di** received her B.S. degree in 2017 from Nanjing Normal University, China. She is currently working toward her M.S. degree in the School of Computer and Communication Engineering, University of Science and Technology Beijing, China. Her research interests include aeronautical communications, cooperative communications and routing algorithm.

**Dingming Liu** is currently working toward his B.S. degree in the School of Computer and Communication Engineering, University of Science and Technology Beijing, China.

**Huansheng Ning** received the B.S. degree from Anhui University in 1996 and the Ph.D. degree in Beihang University in 2001. From 2002 to 2003, he was with Aisino Co. From 2004 to 2013, he was an Associate Professor with the School of Electronic and Information Engineering, Beihang University. Since 2013, he has been a Professor and the Vice Dean with the School of Computer and Communication Engineering, University of Science and Technology Beijing. He has published more than 70 journal/conference papers. His research interests include cybermatics, the Internet of Things, and cyber-physical social systems. He is an IEEE Senior Member, the Founder and the Chair of Cybermatics and Cyberspace International Science and Technology Cooperation Base. He has served as an associate editor for many well reputed journals.